

# Heart Rate Variability in Passive Tilt Test: Comparative Evaluation of Autoregressive and FFT Spectral Analyses

FABIO BADILINI, PIERRE MAISON-BLANCHE, and PHILIPPE COUMEL

From the Department of Cardiology, Hôpital Lariboisière, Paris, France

**BADILINI, F., ET AL.: Heart Rate Variability in Passive Tilt Test: Comparative Evaluation of Autoregressive and FFT Spectral Analyses.** *The dynamic response of the autonomic nervous system during tilting is assessed by changes in the low (LF) and high frequency (HF) components of the RR series power spectral density (PSD). Although results of many studies are consistent, some doubts related to different methodologies remain. Specifically, the respective relevance of autoregressive (AR) and fast Fourier transform (FFT) methods is often questioned. Beat-to-beat RR series were recorded during 90° passive tilt in 18 healthy subjects (29 ± 5 years, eight females). FFT-based (50% overlap, Hanning window) and AR-based (Levinson-Durbin algorithm) PSDs were calculated on the same RR intervals. Powers in very low frequency (VLF: < 0.04 Hz), LF (0.04–0.15 Hz), and HF (0.15–0.40 Hz) bands were calculated either by spectrum integration (FFT and AR<sub>IN</sub>), by considering the highest AR component in each band (AR<sub>HP</sub>), or by summation of all AR components (AR<sub>AP</sub>). LF and HF raw powers (ms<sup>2</sup>) were normalized by total power (%P) and by total power after removal of the VLF component (nu). AR and FFT total powers were not different, regardless of body position. In supine condition, when compared to AR<sub>HP</sub> and AR<sub>AP</sub>, FFT underestimated VLF and overestimated LF, whereas in tilt position FFT overestimated HF and underestimated LF. However, supine/tilt trends were consistent in all methods showing a clear reduction of HF and a less marked increase of LF. Both normalization procedures provided a significant LF increase and further magnified the HF decrease. Results obtained with AR<sub>IN</sub> were remarkably close to those obtained with FFT. In conclusion, significant differences between AR and FFT spectral analyses do exist, particularly in supine position. Nevertheless, dynamic trends provided by the two approaches are consistent. Normalization is necessary to evidence the LF increase during tilt. (PACE 1998; 21:1122–1132)*

**heart rate variability, spectral analysis, tilt test**

## Introduction

Since the original work of Akselrod et al.,<sup>1</sup> spectral analysis of beat-to-beat fluctuations in RR interval has been applied to most of the pathological conditions related with the cardiovascular and autonomic nervous systems. Studies in the literature include investigations on postmyocardial infarction,<sup>2–5</sup> heart failure,<sup>6</sup> coronary artery dis-

ease,<sup>7,8</sup> hypertensive cardiomyopathy,<sup>9</sup> and ventricular tachycardia or fibrillation.<sup>10–12</sup>

The main assumption of spectral analysis of heart rate variability (HRV) is that, like many other biological signals, the time series associated with the heart rate is characterized by oscillatory patterns of different frequency. Two main oscillations are present in HRV signals, namely, a low frequency (LF) and a high frequency (HF) component, which for the human heart are centered at about 0.1 and 0.25 Hz, respectively. A third component of very low frequency (VLF) centered around 0.005 Hz is also often considered, although its physiological origin is less clear.

In the context of short-term HRV signals (in the range of a few minutes), two methods mainly had been used. The first is based on the Fourier transformation of the HRV signal obtained with

Dr. Badilini is supported by a grant from Marquette Electronics Inc., Milwaukee, WI, USA.

Address for reprints: Fabio Badilini, Ph.D., Hôpital Lariboisière, Service de Cardiologie du Prof. Coumel, 2, Rue Ambroise Paré, 75010 Paris, France. Fax: 33-1-49-95-84-39; E-mail: badilini@aol.com

Received February 20, 1997; revised May 5, 1997; accepted May 15, 1997.

the fast Fourier transformation (FFT) algorithm. The second method makes the further assumption that an HRV signal can be described by an autoregressive (AR) model. After having successfully verified such hypothesis, the power spectrum is calculated on the basis of the AR model parameters.

Both LF and HF powers can be calculated as raw values (i.e., the power within each of the bands)<sup>1,3,8,10,11,13-15</sup> or normalized with respect to either the total power (TP) (fractional percent power or %P)<sup>6,16</sup> or the total power minus the VLF component (normalized unit or nu).<sup>7,11,17,18</sup>

The choice of raw or normalized units can lead to different results<sup>6,19</sup> and then must be handled carefully. In addition, a detailed review of the literature shows that studies based on FFT generally use raw powers (with the noticeable exception of Saul et al.<sup>6</sup>), whereas all AR related investigations consistently proposed normalization (either %P or more recently nu). Due to this unexplained circumstance, it is often wrongly believed that normalization may be specific to the methodology implemented. Thus, one may think that the outcome of an experiment is strongly associated with the method used for its achievement. As a final dangerous consequence, the users of one or the other method are often in confrontation,<sup>20,21</sup> and the whole significance of spectral HRV sometimes is questioned.

Regardless of the normalization procedure, the possible differences arising from the application of AR and FFT-based power spectral density (PSD) estimation have never been fully investigated. The main goals of this study were: (1) to apply both AR and FFT spectral analysis in the context of continuous ECG recording during passive tilt test; and (2) to compare raw, fractional, and normalized LF and HF powers obtained with the two methods.

## Methods

### Study Population

The study population consisted of 18 young healthy volunteer subjects (age  $29 \pm 5$  years, eight females). No subject had a history of cardiac disease, hypertension, or diabetes mellitus. None had a prior history of syncope or was receiving medications known to affect the autonomic nervous

system. Inclusion criteria required normal physical examination, blood pressure, and resting ECG in sinus rhythm. All volunteers provided a written informed consent.

### Data Acquisition and Analysis

All tests were performed at about 3:00 p.m. All subjects were instructed to consume a light lunch without alcohol or caffeine and to avoid smoking. The temperature of the room was between 22° and 24°C. Subjects were placed on an electrically driven tilt table, and the ECG was monitored by a three-lead analog Holter recorder (Marquette 8500, Marquette Electronics Inc., Milwaukee, WI, USA). During the entire procedure, subjects were instructed to breathe concurrently with an auditory signal sound at a fixed rate of 15 cycles/min (0.25 Hz). After approximately 15 minutes in the supine position, the table was rotated to a 90° upright position that was maintained for another 15 minutes. None of the volunteers experienced syncope or any symptoms.

Analog data was successively digitized at 128 Hz with a resolution of 10 bits (Marquette Laser Holter system) and transferred to a personal computer for analysis. ECG digital files were first analyzed by a system that identified each QRS complex with first-derivative adaptive threshold algorithm and estimated the apex of the R wave after parabolic interpolation.<sup>22</sup> The continuous series of RR interval were then visualized, and stable 5-minute segments before and after the transition were selected for spectral analysis. In particular, post-tilt data segments always started within 30 seconds after tilt onset and range of interindividual variations was very small (in the range of seconds). No premature beats were observed in the complete set of ECGs; therefore, there was no need for ectopies interpolation. PSD was performed with the Burdick-DMI software (Burdick Inc., Milton, WI, USA).

### FFT-Based Spectral Density

The FFT power spectrum was calculated with the method of averaged Periodogram, also called the Welch Periodogram.<sup>23,24</sup> According to this approach, the original time series to be analyzed was first divided into a number of overlapping subsegments. Percent overlap was fixed to 50%. After

windowing and mean value (DC) subtraction, a Periodogram for each of these subsegments was calculated. At the end of the procedure, the  $N$  Periodograms were averaged. The size of each subsegment was fixed to 128; then,  $N$  was the number of 128 RR sequences (50% overlapped) that could fit in the selected 5-minute period and varied between 3 and 5 (in supine position) and between 3 and 6 (during tilt). Windowing was achieved with a standard Hanning window, which included a correcting coefficient to account for loss of variance.<sup>25,26</sup> Power within specific bands was calculated by integration (area under PSD curve) obtained with trapezoidal rule.

### AR Spectral Density

The estimation of PSD with AR modelization is based on two separate steps: the identification of the model parameters and the calculation of the spectrum on the basis of these parameters.<sup>27,28</sup> The choice of the proper order is very important, as it determines the shape of the power spectrum and it is generally obtained with optimization criteria.<sup>29</sup> In this study, the identification of the model was achieved with a recursive Levinson-Durbin algorithm for the determination of model parameters<sup>30</sup> and Akaike criterion for the choice of model order.<sup>31</sup> Linear detrending was performed before AR modelization. To avoid FFT differences related to preprocessing, we were careful to verify the slope of the trend being very close to 0 (i.e., the detrend was essentially a mean value subtraction) and cases that did not match this condition were not included in the study.

With AR, the global spectrum can be decomposed in a number of spectral components, each one characterized by a bell shape, i.e., by a peak with its own central frequency. As opposed to FFT, the power of a band is not calculated with integration but rather by adding all the single components whose central frequencies are within the band limits. Of note, all the power of a component is assigned to the band its central frequency belongs to, even if the component itself may leak out of the band range.

Despite the pictorial representations of many articles implementing AR that systematically show nice spectra with only three peaks, we often obtain more than one LF or HF component (due to

an effective complexity of the tachogram) or even components with negative powers (due to an overestimation of the model order<sup>32</sup>). In this situation, the LF or HF central frequency corresponds to the highest peak.

In this comparative study between two spectral approaches, the AR power was calculated in three different ways:

1. AR<sub>HP</sub>: Retain only the most important component (the one with highest peak) within each band.
2. AR<sub>AP</sub>: Add all components within each band (the AR gold standard).
3. AR<sub>IN</sub>: Integration (same way of FFT) of overall PSD.

AR<sub>IN</sub> is actually a poor way to use AR-based spectral analysis, and we are not aware whether it has ever been applied. The only rationale for its use in this work is for comparison with FFT, whose *only* way to calculate power is by spectrum integration. Figure 1 shows a schematic example of an AR spectrum.

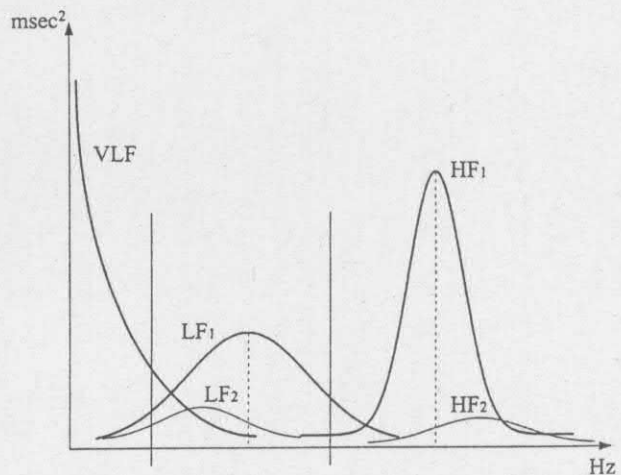


**Figure 1.** Schematic representation of autoregressive power spectral density. In this example, five spectral components are depicted, one in the very low frequency (VLF) band (centered at 0 Hz), two low frequency components (LF<sub>1</sub> and LF<sub>2</sub>), and two in high frequency components (HF<sub>1</sub> and HF<sub>2</sub>). The LF and HF central frequencies are indicated with dashed vertical lines and correspond to the frequencies of highest peaks within each bands (i.e., central frequencies of LF<sub>1</sub> and HF<sub>1</sub>, respectively). The global spectrum is the sum of all five components (not represented in the figure).

### Frequency Ranges for VLF, LF, and HF

Frequency ranges were as follows: VLF:  $\leq 0.04$ ; LF: 0.04–0.15 Hz; and HF: 0.15–0.4 Hz.

### Choice of Type of Tachogram

When dealing with HRV, two kinds of beat-to-beat time series can be used<sup>33</sup>: the time series of measured RR intervals considered to be equidistantly spaced (by a beat event) and the time series consisting of delta spikes nonequidistantly spaced over the time axis (i.e., the distances between spikes is the series of RR intervals). The spectra obtained by using these two approaches are named interval spectrum and spectrum of counts, respectively. The main difference between the two types of spectra resides into their frequency units; in the case of interval spectrum the frequency directly obtained by FFT is cycles/beat (c/b) whereas in the second case it is hertz (Hz). In the first case the c/b units can be remapped to Hz by dividing by the average RR interval. DeBoer et al.<sup>33</sup> clearly demonstrated that the autospectra of the two methods are equivalent.

Many FFT-based studies have used the interval spectrum.<sup>1,34–37</sup> In addition, due to the fact that the AR equation is applied in the "beat" domain, all AR-based works systematically implemented the interval spectrum.<sup>16,28,38,39</sup> Thus, we used the interval spectrum.

Recently, a third type of tachogram that interpolates the nonequidistant RR interval had been developed. This kind of procedure is particularly suitable for long time series where the remapping procedure from c/b to Hz becomes inappropriate.<sup>40–42</sup> To our knowledge, the interpolated tachogram has never been applied for AR methods, as its implementation would have a great deal of consequences on many parameters of AR modelization and it cannot be considered very practical (even though the ESC/NASPE task force does not exclude its implementation<sup>29</sup>). For this reason, resampled tachogram was not considered in this work.

### Length of Tachogram

In order to optimize the comparison, the FFT and AR spectra were calculated on the same RR sequences. In this regard, the AR method is much more flexible as it can be applied to any data

length, whereas the FFT-based method is limited by the power-of-two constrain. Thus, the FFT-based PSD was applied first and the exact number of RR intervals used was stored. Then the AR approach was applied on exactly the same RR time series.

### Raw Powers and Normalized Powers

All raw powers (TP, VLF, LF, and HF) obtained with FFT and the three AR approaches were compared. As far as normalization was concerned, both the fractional percent power (i.e., each component is divided by TP) and the normalized units (i.e., each component is divided by TP - VLF) were applied. The LF/HF ratio (which is independent of normalization) was also compared.

### Statistical Analysis

Raw and normalized powers obtained with FFT and AR approaches were compared with the paired Wilcoxon test. Within each approach, differences between supine and tilt values were also compared with the paired Wilcoxon test.  $P < 0.05$  was considered significant.

### Results

Supine and tilt comparisons between FFT and AR are summarized in Tables I and II and Figure 2.

#### Supine Position (Table I)

Total power was not different between FFT and AR ( $2,057 \pm 1,142$  vs  $2,111 \pm 1,163$  ms<sup>2</sup>, respectively). Of note, all three AR modes of calculation give the same value of TP.

#### Raw Powers

AR<sub>HP</sub> and AR<sub>AP</sub> mean VLF components were significantly larger than the respective values obtained with integration related methods (FFT and AR<sub>IN</sub>). For instance, the mean value of VLF raw power with AR<sub>AP</sub> was  $809 \pm 674$  versus  $565 \pm 528$  ms<sup>2</sup> with FFT ( $P < 0.01$ ). Conversely, mean LF raw powers provided by AR<sub>HP</sub> and AR<sub>AP</sub> were smaller than those of FFT and AR<sub>IN</sub> ( $529 \pm 654$  vs  $683 \pm 373$  ms<sup>2</sup> for AR<sub>AP</sub> and FFT, respectively,  $P < 0.01$ ). In the supine position, raw HF powers were less dependent on the spectral method; a sig-

**Table I.**  
Supine Position (RR = 922 ± 75 ms)

	FFT	AR <sub>HP</sub>	AR <sub>AP</sub>	AR <sub>IN</sub>
TP (ms <sup>2</sup> )	2057 ± 1142	2111 ± 1163	2111 ± 1163	2111 ± 1163
VLF (ms <sup>2</sup> )	562 ± 528	898 ± 880*	809 ± 674*	643 ± 472
LF (ms <sup>2</sup> )	683 ± 373	489 ± 352*	529 ± 674*	632 ± 354
HF (ms <sup>2</sup> )	738 ± 612	609 ± 532*	704 ± 552	760 ± 672
LFnu	47 ± 14	40 ± 15†	42 ± 16†	45 ± 12
LF%P	34 ± 11	26 ± 18†	28 ± 19†	30 ± 10†
HFnu	48 ± 13	44 ± 16†	52 ± 15†	50 ± 12†
HF%P	36 ± 14	29 ± 12†	34 ± 14	35 ± 14
LF/HF	1.15 ± 0.68	1.16 ± 1.26	1.04 ± 1.23	1.02 ± 0.53

\* P < 0.01; † P < 0.05 when compared to fast Fourier transformation (FFT).

nificant difference was only observed when comparing FFT and AR<sub>HP</sub>.

#### Normalized Powers

Logically, fractional powers were consistently smaller than the respective nu powers. For fractional powers, since the denominator of normalization (total power alone) is nearly identical in FFT and AR, all comparisons followed the raw powers tendency (for AR<sub>AP</sub>, LF%P was smaller and HF%P was equivalent, compared to FFT). On the contrary, as they also involved a division by a VLF dependent term, nu powers did not strictly

follow the respective raw powers results; in particular, HFnu in AR<sub>AP</sub> (with higher VLF raw powers) became significantly larger than HFnu in FFT (with smaller VLF raw powers).

#### AR<sub>IN</sub> Versus FFT

In the last column of Table I, the data obtained by using integration on global AR spectrum (AR<sub>IN</sub>) is given. When compared to FFT, AR<sub>IN</sub> raw powers did not show significant differences (closest to significance was LF, P = 0.06). Only two of normalized powers presented significance (LF%P and HFnu).

**Table II.**  
Standing Position (RR = 719 ± 99 ms)

	FFT	AR <sub>HP</sub>	AR <sub>AP</sub>	AR <sub>IN</sub>
TP (ms <sup>2</sup> )	1900 ± 1701	1882 ± 1361	1882 ± 1361	1882 ± 1361
VLF (ms <sup>2</sup> )	676 ± 551	545 ± 585	537 ± 584	723 ± 531
LF (ms <sup>2</sup> )	966 ± 948	1170 ± 1328	1176 ± 1327	902 ± 660
HF (ms <sup>2</sup> )	190 ± 264	102 ± 87	116 ± 88	177 ± 208
LFnu	78 ± 9	81 ± 13	81 ± 13	78 ± 8
LF%P	50 ± 14	55 ± 27	55 ± 27	48 ± 12
HFnu	15 ± 6	11 ± 7*	13 ± 8*	15 ± 5
HF%P	9 ± 4	6 ± 2*	7 ± 4*	9 ± 4
LF/HF	6.56 ± 4.45	12.07 ± 8.99	10.62 ± 8.24*	6.47 ± 3.7

\* P < 0.01 when compared to fast Fourier transformation (FFT).

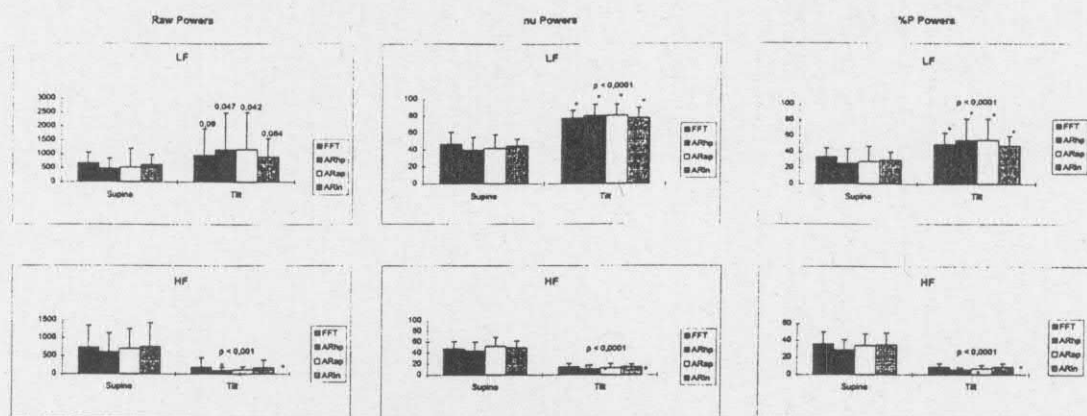


**Figure 2.** Effect of tilting in raw and normalized powers. In each panel, vertical bars and vertical lines indicate means and standard deviation of the power considered, respectively. Statistical significance levels between supine and tilt positions are given. FFT = fast Fourier transformation; HF = high frequency; LF = low frequency.

### Tilt Position (Table II)

As in the supine position, no differences were found when comparing total powers ( $1900 \pm 1701$  vs  $1882 \pm 1361$  ms<sup>2</sup>, respectively, for FFT and AR).

#### Raw Powers

As opposed to the supine position, no significant differences were found between FFT and AR. However, FFT provided increased HF powers close to significance when compared to AR<sub>HP</sub> and AR<sub>AP</sub> ( $190 \pm 64$  vs  $102 \pm 87$  ms<sup>2</sup>, respectively, for FFT and AR<sub>HP</sub>,  $P = 0.056$ ). In addition, mean LF raw powers provided by AR<sub>HP</sub> and AR<sub>AP</sub> tended to be larger than those of FFT and AR<sub>IN</sub> ( $1176 \pm 1327$  vs  $966 \pm 948$  ms<sup>2</sup> for AR<sub>AP</sub> and FFT, respectively,  $P < 0.067$ ).

#### Normalized Powers

As in the supine position, fractional powers were smaller than respective nu powers. With respect to FFT versus AR comparison, all normalized powers followed the raw power tendencies. In addition, all the HF normalized powers of AR<sub>HP</sub> and AR<sub>AP</sub> reached statistical difference when compared to FFT. For instance, mean value of HFnu with AR<sub>AP</sub> was  $13 \pm 8$  versus  $15 \pm 6$  nu with FFT ( $P < 0.01$ ).

#### AR<sub>IN</sub> Versus FFT

No differences were observed, both in raw and normalized powers.

### Supine Versus Tilt (Fig. 2)

As typically observed with this test, the RR interval significantly decreased (from  $922 \pm 75$  to  $719 \pm 99$  ms;  $P < 0.0001$ ).

#### Raw Powers

The comparisons between supine and tilt positions provided homogenous results with all four approaches. Specifically, mean TP and VLF powers did not change with all approaches. Raw LF powers did increase in all methods, but significance levels were consistently in the borderline region ( $P = 0.09, 0.047, 0.042,$  and  $0.084$  for FFT, AR<sub>HP</sub>, AR<sub>AP</sub>, and AR<sub>IN</sub> respectively). Conversely, the decrease of raw HF powers was apparent ( $P < 0.001$  for all methods).

#### Normalized Powers

With both normalization procedures, LF powers increased significantly ( $P < 0.0001$  in all methods), and all HF normalized powers decreased significantly ( $P < 0.0001$  in all methods). Figure 3 shows the FFT and AR PSDs of a subject in the supine and tilt positions.

### Discussion

This is the first study in which FFT and AR approaches were applied to the same population

in the context of passive tilt test. Two main findings have to be highlighted: (1) within all frequency bands, powers provided by the two methods can show substantial differences, especially in the supine position; and (2) trends provided by the two methods are equivalent.

Another important contribution is the direct comparison between two methods of normalization. In this regard, both normalized units and percent of total power are able to highlight the increase of LF. On the contrary, the decrease of HF is already obvious in the raw powers and simply is magnified with both normalization procedures.

**Difference in Raw Powers: Tail Effect?**

The understanding of the possible differences between the two methods is not simple. However, the striking similarity between FFT and AR<sub>IN</sub> suggests that the differences may be the effect of the way the power within a band is computed. With FFT and AR<sub>IN</sub>, the power is calculated by integration of the spectrum between the band lower and upper limits. Conversely, with standard AR (AR<sub>HP</sub> or AR<sub>AP</sub>), the criteria of assignment is only based on the central frequency value of a well-defined oscillatory pattern. Thus, when two neighboring components are considered, the tails of each component could be assigned to one or another band

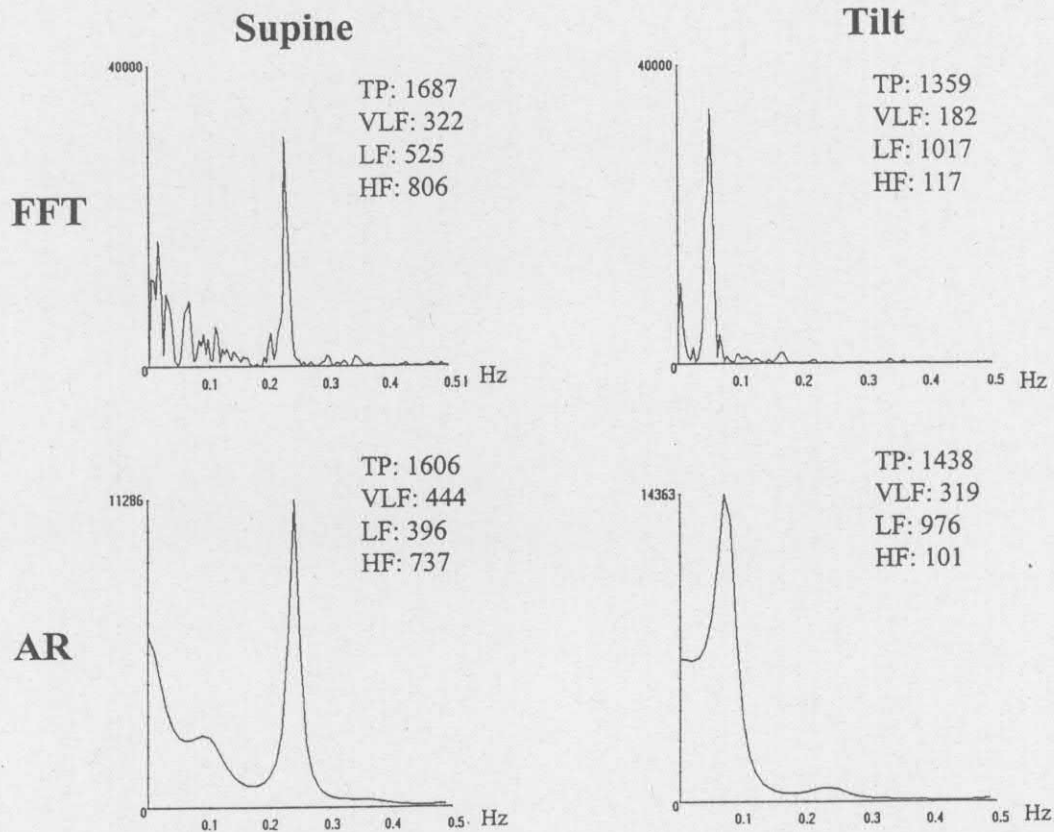


**Figure 3.** Fast Fourier transformation (FFT) and autogressive (AR) power spectral densities (PSDs) in a representative subject. Upper and lower panels show the FFT-based and the AR-based PSDs (left side for supine position and right side for tilt position). The typical smoothed shape of the AR spectrum is apparent. Raw powers of total power (TP), very low frequency (VLF), low frequency (LF), and high frequency (HF) are also given for all four plots (all values in ms<sup>2</sup>). AR data have been obtained by adding all components (AR<sub>AP</sub>). In this subject, VLF decreases between supine and tilt.

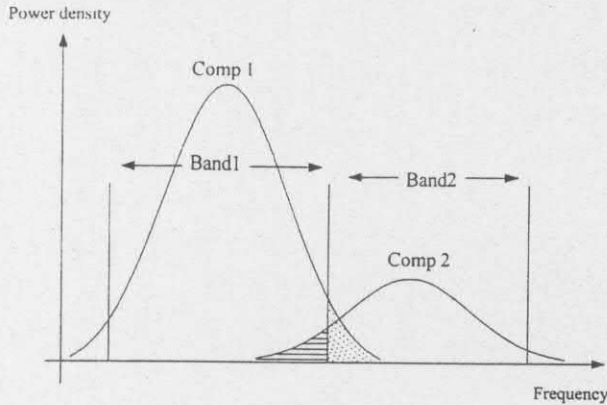


**Figure 4.** Schematic representation of component tail effect. The power density of two neighboring components (Comp1, Comp2) are shown. Vertical lines mark the cut-off limits of two adjacent bands (Band1, Band2). The dashed line area indicates the tail of Comp1 outside the upper limit of Band1, and the solid line area identifies the tail of Comp2 outside the lower limit of Band2. FFT and  $AR_{IN}$  would assign dashed line area to Band2 and solid line area to Band1, whereas standard AR would have done the opposite. The position of the adjacent cutoff and the respective size of the neighboring components determine the magnitude of the tail effect.

depending on the method used. A schematic representation of this situation is shown in Figure 4.

In the supine position, VLF is a dominant component (Table I). Then, with FFT and  $AR_{IN}$  the large tail of VLF is lost, resulting in a smaller value. Consequently, the neighboring LF is largely overestimated by FFT and AR integration. Total powers (which are not concerned by the power integration mode) are identical. The typical supine spectrum is idealized in Figure 5.

In the standing position, LF becomes predominant, particularly with respect to HF (Table II), which is then overestimated by FFT and  $AR_{IN}$ . The typical spectrum obtained in the standing position is idealized in Figure 6.

In order to better quantify this phenomenon, we calculated the percent changes of raw powers between  $AR_{AP}$  and  $AR_{IN}$ . In the supine position, 15 subjects had a larger  $AR_{IN}$  LF raw power (global mean value of increase:  $15\% \pm 17\%$ ) and 17 subjects had a smaller  $AR_{IN}$  VLF raw power (global mean value of decrease  $23\% \pm 23\%$ ). In

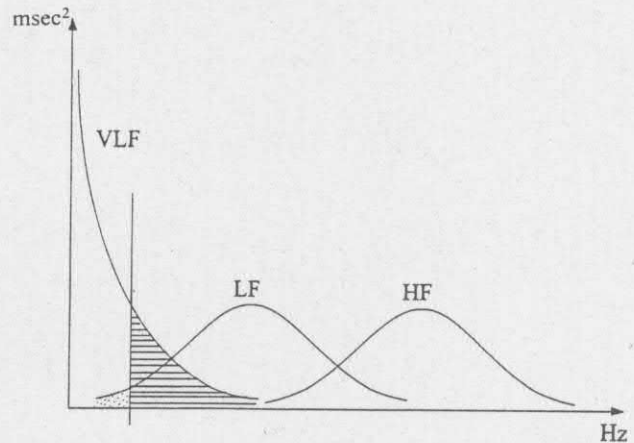


**Figure 5.** Schematic representation of typical supine position spectrum. Vertical line indicates the cutoff between very low frequency (VLF) and low frequency (LF) bands. The overestimation of LF component by FFT and  $AR_{IN}$  is the result of the big VLF tail (solid line area), which by integration is assigned to the LF band. HF = high frequency.

the standing position, 16 subjects had a larger  $AR_{IN}$  HF raw power (global mean value of increase:  $39\% \pm 44\%$ ). All other percent changes (i.e., HF in supine, VLF and LF in standing) did not show consistent variations in one specific direction.

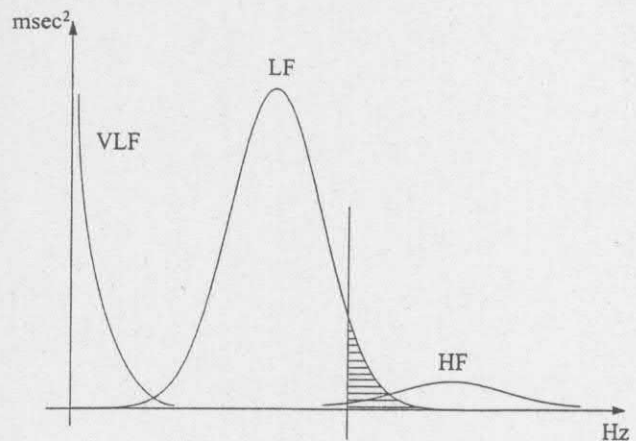


**Figure 6.** Schematic representation of typical tilt position spectrum. Vertical line indicates the cutoff between low frequency (LF) and high frequency (HF) bands. The overestimation of HF component by FFT and  $AR_{IN}$  is the result of the big LF tail, which by integration is assigned to the HF band. VLF = very low frequency.



## Trends

Despite the observed differences in the raw powers, the dynamic information provided by the two approaches is consistent. Specifically, HF power significantly decreases following passive tilting, either by considering raw or normalized powers. On the contrary, the increase of raw LF power is less consistent, being close to significance with all methods, and becomes apparent only after normalization (Fig. 2).

These results are in accordance with findings of Montano et al.<sup>19</sup> using an AR approach. What we can add is that the less evident increase of LF is not related to the spectral method. The pathophysiological explanation of both LF and HF components and the speculations over sympathetic excitation versus vagal withdrawal during tilt are not the purpose of this study; however, we can highlight that the main effect of tilt seems to be the reduction of HF (which in the average is reduced by 6×) rather than the increase of LF (which in the average is only doubled).

Both methods did not show evidence of any change in mean VLF powers following passive tilting, thus indicating that this component should not play a role in this kind of test. In addition, the individual behavior was rather erratic, as raw VLF increased in 10 (of 18) subjects and fractional VLF increased in 13 subjects. A detailed review of the literature did not provide quantitative data on the behavior of this component during orthostatic test, either because it was totally ignored,<sup>13,15,16</sup> considered as pure direct current component,<sup>2</sup> or because raw data were not provided.<sup>19</sup> The recent ESC/NASPE document addresses a note of caution on the physiological explanation of VLF<sup>29</sup>; yet, in the only two quantitative examples available from two figures, the VLF power showed an apparent decrease.

Finally, total powers are also unchanged by tilt maneuver. This finding is in accordance with some studies<sup>13,15</sup> and is in disaccordance with others.<sup>16,19</sup> Nevertheless, by eliminating the four largest outliers, the (recalculated) total powers were  $1,852 \pm 832$  and  $1,207 \pm 543$  ms<sup>2</sup> (for supine and standing positions, respectively), and the comparison became significant ( $P = 0.02$ ). These values are much closer to those obtained by Pagani et al.<sup>16</sup> on a similar population and suggests

how discordances in literature may be associated to the different populations and to the large inter-variability between subjects.

## Normalization Procedures

In the most general situation, the need for normalization is essentially justified by the large differences that can be found in the total powers being compared. This can be particularly valid when the populations analyzed include different pathological groups<sup>6,7,12</sup>; however, even within the same population and with a simple maneuver such as tilt, large interindividual variations in power can lead to confounding interpretations. In spite of the lack of difference observed in the total powers (see preceding paragraph), our data also indicated the presence of a large range of total power (486–5049 and 202–7276 ms<sup>2</sup> for supine and standing positions, respectively), as shown by the standard deviations of Figure 2.

With respect to different procedures, normalization by the total power alone clearly supplies smaller values than normalization over total power minus VLF (Fig. 2, Tables I and II). Despite this legitimate difference, both normalization procedures were able to highlight the decrease of HF and most of all the increase of LF. The normalization to choose cannot be restricted to that which better denotes the supine/tilt changes but rather depends on the interpretation we want to give to the VLF power. If the power within this band is really of nonphysiological origin and comes from artifactual components,<sup>19</sup> the normalized units may be preferable. If, on the contrary, VLF may contain information, its use in the normalization procedure may introduce a bias. Given the results of this work, which did not suggest a physiological explanation of VLF in the tilt test, normalized units seem to be the right choice and the introduction of possible biases should be excluded.

## Conclusion

AR and FFT spectral analyses provide different quantitative results. Differences between the two methodologies may depend on subject position and

may be explained by the mode of spectrum integration specific of each approach. Nevertheless, the qualitative assessment of sympathovagal changes in the context of passive tilt testing is accurately iden-

tified by both techniques. Normalization procedures that do or do not account for VLF powers are capable of showing a significant increase of LF and magnifying an already significant decrease of HF.

## References

1. Akselrod S, Gordon D, Ubel FA, et al. Power spectrum analysis of heart rate fluctuation: A quantitative probe of beat-to-beat cardiovascular control. *Science* 1981; 213:220-222.
2. Lombardi F, Sandrone G, Pernpruner S, et al. Heart rate variability as an index of sympathovagal interaction after myocardial infarction. *Am J Cardiol* 1987; 60:1239-1245.
3. Bekheit S, Tangella M, el-Sakr A, et al. Use of heart rate spectral analysis to study the effects of calcium channel blockers on sympathetic activity after myocardial infarction. *Am Heart J* 1990; 119:79-85.
4. Bigger JT, Fleiss JL, Steinman RC, et al. Frequency domain measures of heart period variability and mortality after myocardial infarction. *Circulation* 1992; 85:164-171.
5. Bigger JT, Fleiss JL, Rolnitzky LM, et al. Frequency domain measures of heart period variability to assess risk late after myocardial infarction. *J Am Coll Cardiol* 1993; 21:729-736.
6. Saul JP, Aray Y, Berger RD, et al. Assessment of autonomic regulation in chronic congestive heart failure by heart rate spectral analysis. *Am J Cardiol* 1988; 61:1292-1299.
7. Huikuri HV, Niemelä MJ, Ojala S, et al. Circadian rhythms of frequency domain measures of heart rate variability in healthy subjects and patients with coronary artery disease. *Circulation* 1994; 90:121-126.
8. Yoshio H, Shimizu M, Sugihara N, et al. Assessment of autonomic nervous activity by heart rate spectral analysis in patients with variant angina. *Am Heart J* 1993; 125:324-329.
9. Counihan PJ, Fei L, Bashir Y, et al. Assessment of heart rate variability in hypertrophic cardiomyopathy: Association with clinical and prognostic features. *Circulation* 1993; 88:1682-1690.
10. Myers GA, Martin GJ, Magid NM, et al. Power spectral analysis of heart rate variability in sudden cardiac death: Comparison to other methods. *IEEE Trans Biomed Eng* 1986; 33:1149-1156.
11. Huikuri HV, Valkama JO, Airaksinen KEJ, et al. Frequency domain measures of heart rate variability before the onset of nonsustained and sustained ventricular tachycardia in patients with coronary artery disease. *Circulation* 1993; 87:1220-1228.
12. Fei L, Anderson MH, Statters DJ, et al. Effects of passive tilt and submaximal exercise on spectral heart rate variability in ventricular fibrillation patients without significant structural heart disease. *Am Heart J* 1995; 129:285-280.
13. Lipsitz LA, Mietus J, Moody GB, et al. Spectral characteristics of heart rate variability before and during postural tilt. *Circulation* 1990; 81:1803-1810.
14. Morillo CA, Klein GJ, Jones DL, et al. Time and frequency domain analyses of heart rate variability during orthostatic stress in patients with neurally mediated syncope. *Am J Cardiol* 1994; 74:1258-1262.
15. Vybiral T, Bryg RJ, Maddens ME, et al. Effect of passive tilt on sympathetic and parasympathetic components of heart rate variability in normal subjects. *Am J Cardiol* 1989; 63:1117-1120.
16. Pagani M, Lombardi F, Guzzetti S, et al. Power spectral analysis of heart rate and arterial pressure variabilities as a marker of sympathovagal interaction in man and conscious dog. *Circ Res* 1986; 59:178-193.
17. Lombardi F, Sandrone G, Mortara A, et al. Circadian variation of spectral indices of heart rate variability after myocardial infarction. *Am Heart J* 1992; 123:1251-1259.
18. Furlan R, Guzzetti S, Crivellaro W, et al. Continuous 24-hour assessment of the neural regulation of systemic arterial pressure and RR variabilities in ambulant subjects. *Circulation* 1990; 81:537-547.
19. Montano N, Gneccchi Ruscone T, Porta A, et al. Power spectrum analysis of heart rate variability to assess the changes in sympathovagal balance during graded orthostatic tilt. *Circulation* 1994; 90:1826-1831.
20. Goldsmith RL, Bigger JT, Steinman RC, et al. Comparison of 24-hour parasympathetic activity in endurance-trained young men. *J Am Coll Cardiol* 1992; 20:552-558.
21. Pagani M, Lombardi F, Malliani A. Heart rate variability: Disagreement on the markers of sympathetic and parasympathetic activities. *J Am Coll Cardiol* 1992; 22:951-953.
22. Merri M, Farden DC, Mottley JG, et al. Sampling frequency of the electrocardiogram for the spectral analysis of heart rate variability. *Trans Biomed Eng* 1990; 37:99-106.
23. Oppenheim AV, Schaffer RW. *Discrete-Time Signal Processing*. Englewood Cliffs, NJ, Prentice-Hall, 1975.
24. Welch PD. The use of Fast Fourier Transform for the estimation of power spectra: A method based on time averaging over short, modified Periodograms. *IEEE Trans Audio Electroac* 1967; 15:70-74.

25. Harris FJ. On the use of windows for harmonic analysis with the Discrete Fourier Transform. *Proc IEEE* 1978; 66:51-83.
26. Badilini F, Maison-Blanche P. HRV spectral analysis by the averaged Periodogram: Does the total power really match with the variance of the tachogram? *Ann Noninvas Electrocardiol* 1996; 1:423-429.
27. Bartoli F, Baselli G, Cerutti S. AR identification and spectral estimate applied to the R-R interval measurement. *Int J Biomed Comput* 1985;16:201-215.
28. Baselli G, Cerutti S, Civardi S, et al. Parameter extraction from heart rate and arterial blood pressure variability signals in dogs for the validation of a physiological model. *Comput Biol Med* 1988; 18:1-16.
29. ESC/NASPE Task Force. Heart rate variability: Standards of measurement, physiological interpretation, and clinical use. Report from the ESC/NASPE Task Force. *Circulation* 1996; 93:1043-1065.
30. Kay SM, Marple SL. Spectrum analysis: A modern perspective. *Proc IEEE* 1981; 69:1380-1419.
31. Akaike H. A new look at the statistical model identification. *IEEE Trans Autom Cont* 1974; 19:716-723.
32. Pinna GD, Maestri R, Di Cesare A. Application of time series spectral analysis theory: Analysis of cardiovascular variability signals. *Med Biol Eng Comput* 1996; 34:142-148.
33. DeBoer R, Karemaker JM, Strackee J. Comparing spectra of a series of point events particularly for heart rate variability data. *IEEE Trans Biomed Eng* 1984; 31:384-387.
34. Chess GF, Tam RMK, Calaresu FR. Influence of cardiac neural inputs on rhythmic variations of heart rate period in the cat. *Am J Physiol* 1975; 228:775-780.
35. Sayers BM. Analysis of heart rate variability. *Ergonomics* 1973; 16:17-32.
36. Mohn RK. Suggestions for the harmonic analysis of point process data. *Comput Biomed Res* 1976; 9:521-530.
37. Kitney RI, Rompelman O. *The Study of Heart Rate Variability*. Oxford, England, Clarendon, 1980, pp. 27-58.
38. Baselli G, Cerutti S, Civardi S, et al. Cardiovascular variability signals: Towards the identification of a closed-loop model of the neural control mechanisms. *IEEE Trans Biomed Eng* 1988; 35:1033-1043.
39. Malliani A, Pagani M, Lombardi F, et al. Cardiovascular neural regulation explored in the frequency domain. *Circulation* 1991; 84:1482-1492.
40. Albrecht P, Cohen RI. Estimation of heart rate power spectrum bands from real-world data: Dealing with ectopic and noisy data. *Comput Cardiol* 1988; 15:311-314.
41. Rottman JN, Steinman RC, Albrecht P, et al. Efficient estimation of the heart period power spectrum suitable for physiologic or pharmacologic studies. *Am J Cardiol* 1990; 66:1522-1524.
42. Bigger JT, Albrecht P, Steinman RC, et al. Comparison of time- and frequency-domain based measures of cardiac parasympathetic activity in Holter recordings after myocardial infarction. *Am J Cardiol* 1989; 64:536-538.